MATERIALS SCIENCE

Acylhydrazine-based reticular hydrogen bonds enable robust, tough, and dynamic supramolecular materials

Yuanxin Deng[1,2]†, Qi Zhang[1,2]†, Chenyu Shi[1], Ryojun Toyoda[2], Da-Hui Qu[1]*, He Tian[1], Ben L. Feringa[1,2]*

Supramolecular materials are widely recognized among the most promising candidates for future generations of sustainable plastics because of their dynamic functions. However, the weak noncovalent cross-links that endow dynamic properties usually trade off materials' mechanical robustness. Here, we present the discovery of a simple and robust supramolecular cross-linking strategy based on acylhydrazine units, which can hierarchically cross-link the solvent-free network of poly(disulfides) by forming unique reticular hydrogen bonds, enabling the conversion of soft into stiff dynamic material. The resulting supramolecular materials exhibit increase in stiffness exceeding two to three orders of magnitude compared to those based on the hydrogen-bonding network of analogous carboxylic acids, simultaneously preserving the repairability, malleability, and recyclability of the materials. The materials also show high adhesion strength on various surfaces while allowing multiple surface attachment cycles without fatigue, illustrating a viable approach how robustness and dynamics can be merged in future material design.

INTRODUCTION

Lengthening the life cycle of polymeric materials, particularly by introducing functionality that allows ready recycling without compromising the key materials properties, provides a major contemporary challenge and represents an urgent goal for the scientific community due to the rapidly rising global problems caused by traditional plastics (*1–3*). Replacing the irreversible covalent bonds in common plastics by dynamic chemical bonds offers a promising solution enabling intrinsically dynamic polymeric materials that can self-repair, be reused, and recycled on our way to future sustainable plastics (*4–9*). The rise of supramolecular polymers, i.e., macromolecules formed by linking small molecules via noncovalent bonds, has sparked the creation and application of a variety of constitutionally dynamic noncovalent materials (*10–11*). The reversible bond dissociation and exchange of noncovalent bonds endow supramolecular materials with unique dynamic functions, however, usually trading off the mechanical robustness and durability of materials due to the inherently weak bond strength of noncovalent cross-links and focused their most frequent uses on soft adaptive materials (*12, 13*), e.g., extracellular matrix of artificial tissue (*14*). To make supramolecular materials truly suitable as replacement for traditional plastics, the fundamental challenge is how to develop robust, simple, and dynamic supramolecular cross-linking strategies that simultaneously enable, apparently contradicting, mechanical durability (robustness) and dynamic behavior (reversibility, disassembly, and repairability) of the polymers.

Hydrogen bonds (H-bonds) are the ubiquitous noncovalent interactions in nature sustaining life itself most obvious in the structures of proteins and DNA and representing the prevalent noncovalent

cross-links for supramolecular polymers (*15–17*). H-bonds are reversible and usually weak, but tailoring the multivalency and directionality of H-bonds, materials cross-linked by H-bonds are accessible that show high mechanical robustness (*17*). A fascinating example created by nature is ice, a stiff supramolecular material completely cross-linked by H-bonds. The robustness of ice originates from the synergy of numerous H-bonds that are present in a reticular network due to the specific geometry of water molecules (*18*). Meanwhile, the highly ordered reticular framework of ice can also heal and reshape itself by dynamic reorganization of the hydrogen bonds through a reversible thaw-freeze process under mild conditions. Combining mechanical robustness and reversibility, we are motivated to explore robust supramolecular tools that offer similarly reticular H-bonding cross-links for polymers to enhance material strength without compromising the dynamic functions.

Here, we report our discovery that a structurally simple unit, i.e., an acylhydrazine, can induce self-assemble into a three-dimensional reticular cross-linking H-bonding network (Fig. 1). Introducing the acylhydrazine cross-links into dynamic disulfide-based polymers results in a simultaneous enhancement of material stiffness (two to three orders of magnitude), toughness, and adhesiveness, compared to those based on the typical H-bonds of carboxylic acids. Meanwhile, the hierarchical reticular H-bond cross-links preserve the intrinsically dynamic functions of poly(disulfides), such as complete repairing, malleability, and reusability under mild conditions. The notable enhancement of material properties brought by a simple molecular design using acylhydrazine units to tune hydrogen bonds demonstrates the power of controlling macroscopic properties of supramolecular materials by precise structural elaboration at the molecular level controlling intermolecular interactions and offers a robust and straightforward cross-linking strategy for designing high-performance yet dynamic materials.

RESULTS AND DISCUSSION
Design of reticular H-bonding self-assembly

The discovery came from our long-lasting research interests in developing self-healable and recyclable supramolecular materials based on

[1]Key Laboratory for Advanced Materials and Joint International Research Laboratory of Precision Chemistry and Molecular Engineering, Feringa Nobel Prize Scientist Joint Research Center, Frontiers Science Center for Materiobiology and Dynamic Chemistry, School of Chemistry and Molecular Engineering, East China University of Science and Technology, 130 Meilong Road, Shanghai 200237, China. [2]Strathclyde Institute for Chemistry and Zernike Institute for Advanced Materials, Faculty of Science and Engineering, University of Groningen, Nijenborgh 4, 9747 AG, Groningen, Netherlands.
*Corresponding author. Email: dahui_qu@ecust.edu.cn (D.-H.Q.); b.l.feringa@rug.nl (B.L.F.)
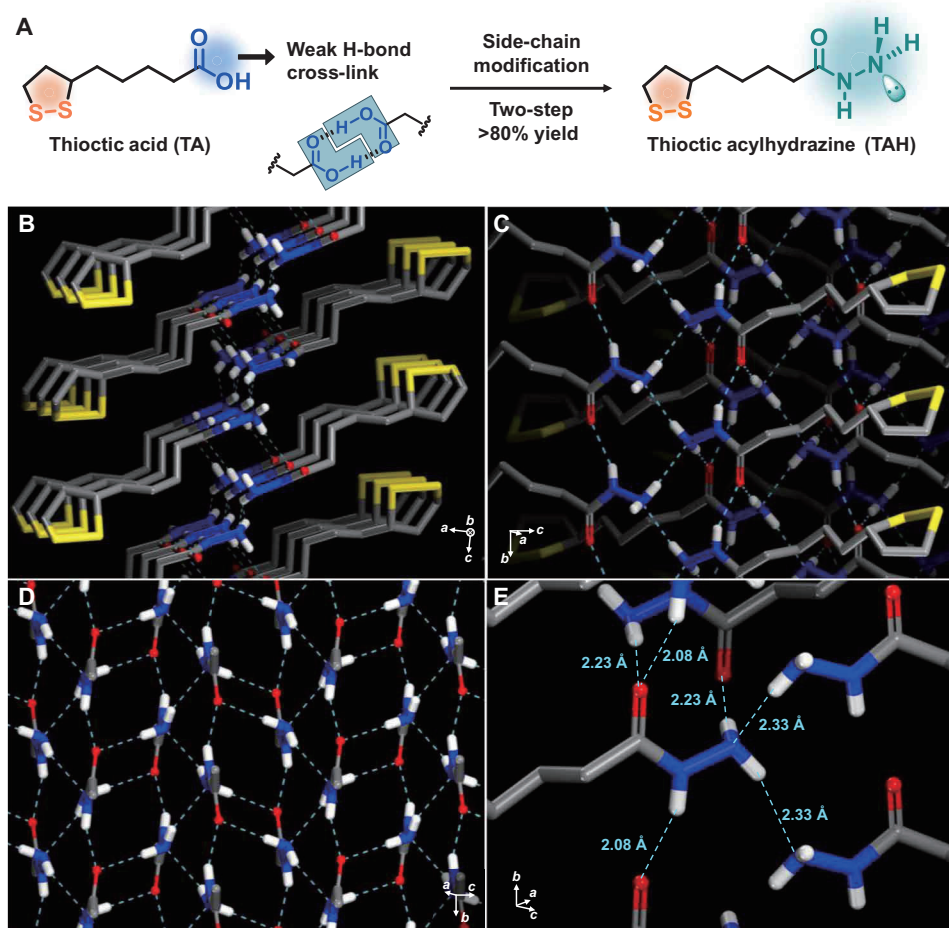†These authors contributed equally to this work.

Fig. 1. Reticular H-bonding cross-links based on acylhydrazine units. (**A**) Sidechain design strategy deriving from TA with dimeric H-bonds to TAH with reticular H-bonds. (**B** to **E**) X-ray single-crystal structure of TAH monomers. View along *b* axis (B) shows the antiparallel molecular self-assembly of TAH mediated by reticular H-bonds. View along *c* axis (C) and view along *a* axis (D) present the geometrically intricate H-bonding network of acylhydrazines (only acylhydrazine groups are shown in Fig. 1D for clear presentation). Insight view (E) shows the atomic structures of an acylhydrazine group bound with six intermolecular H-bonds. Irrelevant hydrogen atoms are omitted for clarity.

thioctic acid (TA) (*19–23*), a natural small molecule that is present as a coenzyme in the body of animals (*24*). The disulfide-containing five-membered ring, with a dynamic covalent S-S bond, can undergo ring-opening polymerization (ROP) in a solvent-free melting state, forming soft and stretchable materials that are mainly cross-linked by the dimeric H-bonds of carboxylic acids (*19*). Although some further cross-links by metal-carboxylate complexes and ionic interactions have been developed to toughen the supramolecular network (*21*), the inherent weakness of the dimeric H-bonds of carboxylic acids limits the mechanical robustness and the practical applications of the resulting materials.

Aiming to evolve the dimeric H-bonds of carboxyl groups into reticular H-bonds, we noticed the structural feature of acylhydrazines (Fig. 1A): A single acylhydrazine unit contains three H-donors and two H-acceptors, meaning that one of the H-acceptors may simultaneously interact with two H-donors so that the global supramolecular system can be stabilized by saturating all the H-donors. Inspired by this hypothesis, we prepared TAH monomers from TA at a large scale (up to 50 g) in a chromatography-free and high-yield (over 85%) single-step procedure (Fig. 1A and figs. S1 to S3). For detailed

procedures and characterizations, see the "Experimental method" section in the Supplementary Materials), affording yellow powders with a melting point of 77°C (fig. S4). The increased melting point from TA (60°C) to TAH (77°C) suggests the presence of multiple H-bonds in TAH solids. To explore the atom-precision self-assembly structure, TAH was crystallized from tetrahydrofuran/heptane solvent mixture (under the strict absence of heat and light to prevent polymerization) providing the single-crystal x-ray structure. Unexpectedly, we discovered a notably complex H-bonding network of acylhydrazine units in the solid state (Fig. 1, B to E, and table S1): (i) The molecules were packed in an antiparallel manner along the *b* axis (Fig. 1B); (ii) The adjacent antiparallel stacks further interacted and cross-linked by forming hydrazine-hydrazine and hydrazine-carbonyl H-bonds, resulting in a reticular framework fully cross-linked by H-bonds (Fig. 1, C and D). In this fascinating architecture, all the H-bond donors and acceptors were saturated by forming H-bonds with varied bond lengths (2.08 to 2.33 Å; Fig. 1E). We also found that the carbonyl groups were "oversaturated" by forming H-bonds with two N–H donors, which may be a key feature responsible for the formation of reticular H-bonding network.

To further understand the hierarchical H-bonding assembly of TAH, infrared spectroscopy (IR; figs. S5 and S6) and temperature-varied nuclear magnetic resonance (NMR; figs. S7 to S13) were used to study the H-bonding status of TAH under concentration-dependent conditions with dichloromethane as the H-bond–supporting solvent. Under high dilution (1 mM), the TAH molecules were mostly molecularly dissolved because of the nonbonded amide band (υ_{N-H} = 3443 cm^{-1}; δ_{N-H} = 1605 cm^{-1}) and the nonbonded carbonyl band ($\upsilon_{C=O}$ = 1678 cm^{-1}) observed in IR spectra (figs. S5 and S6A) and the small temperature-decreasing coefficient [$\Delta\delta/\Delta T$ = −1.7 parts per billion (ppb)/K] (25) of the amide proton in the ^{1}H NMR spectra (figs. S7 to S11). Increasing the concentration drove the formation of intermolecular H-bonding interactions, as shown by the corresponding shift of amide band and carbonyl band (figs. S5 and S6) and the remarkably increased temperature-decreasing coefficient ($\Delta\delta/\Delta T$ = −11.9 ppb/K at 200 mM; fig. S12). The change in the IR spectra from 1 to 200 mM solution and then in the solid state clearly indicated the distinctive shifting of the IR bands of amide N–H and carbonyl groups, confirming the hierarchical mode of the H-bonding self-assembly of TAH. Combining with the bond length analysis based on the x-ray structure (Fig. 1E), we can infer that the amide-amide H-bonds support the primary self-assembly, and the hydrazine-hydrazine and hydrazine-carbonyl H-bonds drive the secondary self-assembly to form the reticular H-bonding network.

To further support the reliability of our H-bond design strategy, two amide analogs of TAH were synthesized and characterized (figs. S14 to S20 and table S2). First, the primary amide (TAA) bears one H-acceptor and two H-donors, i.e., reminiscent of the nonsaturation strategy but with the propensity to form hydrogen bonding distinctly different from TAH featuring two H-acceptor and three H-donors. The x-ray single-crystal structure of TAA showed a reticular H-bonding framework but unlike that of TAH (fig. S20), and, in addition, TAA does not undergo polymerization (vide infra), likely the direct consequence of the distinct H-bonding design. On the other hand, the N,N-dimethyl–substituted analog (TAMH) was an oil and could not be crystallized (figs. S17 to S19), obviously lacking reticular H-bonds as cross-links. The combined results of structural comparison indicated the reliability and generality of our strategy for the design of reticular H-bonding–based self-assembly.

Polymer preparation and characterization

After having established a fundamental insight in the hierarchical reticular H-bonds of TAH in the solid state, we move to the polymerization of TAH to investigate how the acylhydrazine units cross-link in solvent-free polymers. To this end, the disulfide-mediated ROP of TAH monomers was performed under solvent-free melting conditions (Fig. 2, A and B) (see detailed experimental procedures in the "Experimental method" section in the Supplementary Materials). To enable high–molecular weight poly(disulfides), a series of dithiocarbamate (DTC)–based catalysts, including Zn(DTC)$_2$, Na(DTC), and DTC, were used because of their capability of catalyzing the sulfur-sulfur bond exchange reaction in the vulcanization of rubber (fig. S21) (26). The resulting poly(TAH) samples formed without catalysts were translucent solid materials (fig. S22A) with an amorphous network as confirmed by x-ray diffraction (figs. S22B and S23). Notably, it was found that applying Zn(DTC)$_2$ as catalyst led to less translucent samples with visibly enhanced stiffness: A piece of poly(TAH)-5% Zn(DTC)$_2$ network can support a 200-g weight without any deformation (Fig. 2C and movie S1). These intriguing observations triggered

us to investigate how the catalysts affected the structure and properties of the poly(disulfide) network. IR spectra of these solvent-free poly(TAH) with and without catalysts showed broad and consistent vibration bands (υ_{N-H} and $\upsilon_{C=O}$) attributed to TAH monomers (Fig. 2D and figs. S24 to S27), indicating that the acylhydrazine units followed the H-bonding pattern as observed in the x-ray crystal structure (Fig. 1, B to E). On the other hand, according to literature reports (26), DTC-based catalysts can activate disulfide bonds and drive rubber vulcanization reactions. In our system, we inferred that the presence of DTC-based catalysts, especially Zn(DTC)$_2$, notably increased the molecular weight of poly(TAH) polymers because of (i) the remarkably higher glass transition temperature (T_g; figs. S28 to S31), (ii) similar vibration bands of C=O groups in IR spectra (Fig. 2D and figs. S25 to S27) excluding metal-acylhydrazine interactions, (iii) high–molecular weight–induced microphase separation in the presence of catalysts (fig. S32), and (iv) peak distribution in the analysis of gel permeation chromatography (GPC; fig. S33). To illustrate the microphase structure, synchrotron-radiation small-angle x-ray scattering technology was used, exhibiting enhanced broad scattering peaks with increasing amounts of catalysts (fig. S34). The observed microphase separation can be attributed to the secondary clustering of the reticular H-bonded acylhydrazine units in the high–molecular weight solvent-free poly(TAH) network (27). By calculation, applying the Bragg equation, the H-bond clusters were distributed in the network with an average internal distance of 52 nm (fig. S34). Hence, the hierarchical cross-linking topology of the H-bonding network can be easily controlled by varying the addition amounts of Zn(DTC)$_2$ catalysts, which offers us opportunities to tune the macroscopic properties of the H-bonding network of poly(TAH).

The thermal properties of the resulting polymers were further studied by differential scanning calorimetry (DSC) and thermogravimetry (TG). The glass transition temperature (T_g) of poly(TAH) polymers revealed by DSC was found to be positively correlated with the amount of added catalysts (figs. S28 to S31), which should be attributed to two factors; (i) the catalysis-enhanced molecular weight, as supported by GPC analysis (fig. S33), and (ii) the secondary cross-linking of H-bonding clusters that decrease the mobility of polymer chains. The TG curves of all poly(TAH) samples showed high thermostability with similar decomposition temperatures over 200°C (figs. S35 to S37). Despite the fully noncovalent network and excellent solubility of TAH monomers, all the poly(TAH) polymers unexpectedly show to be insoluble in water and many organic solvents (fig. S38), only swelling in methanol and being soluble in dimethyl formamide and dimethyl sulfoxide. The excellent solvent resistance is unusual for supramolecular materials that can be attributed to the robust cross-linking due to the reticular H-bonds of the acylhydrazine units.

Mechanical robustness and toughness

Having established the hierarchically reticular H-bonding of poly(TAH) network, we moved to the key question: How this unique noncovalently cross-linking acylhydrazine unit affects the macroscopic mechanical properties of the materials compared with the traditional dimeric H-bonds, e.g., carboxylic acids. The results of the systematic investigation of the mechanical properties of poly(TAH) materials are compiled in Fig. 2 and figs. S39 to S42. The poly(TAH) polymer without catalyst shows a tensile Young's modulus of 8.0 MPa (Fig. 2E and fig. S39), which was nearly 100-fold higher than our previously reported network mainly cross-linked by carboxylic acids (84 KPa)
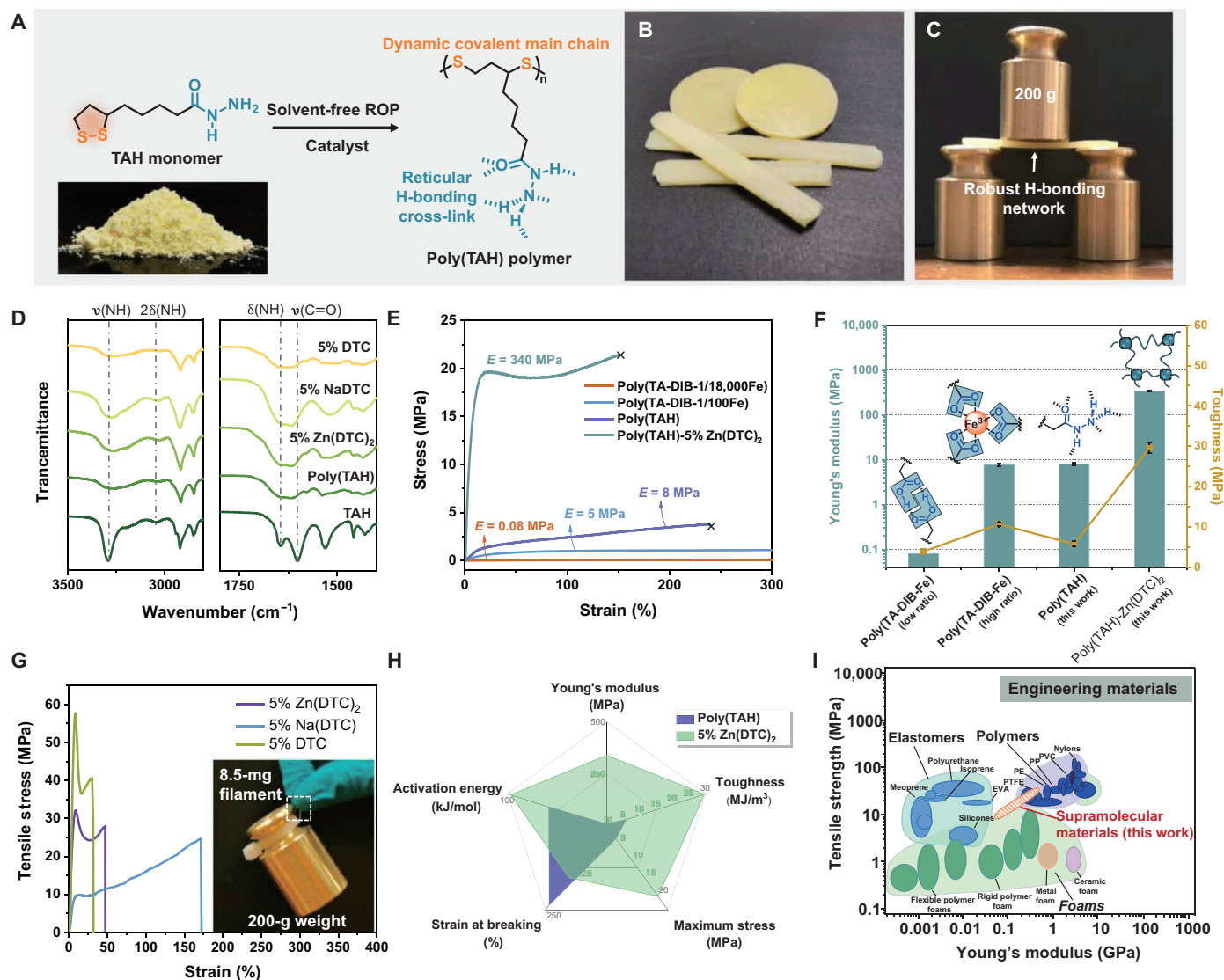
Fig. 2. Structure characterization and mechanical properties of poly(TAH) polymers. (**A**) Preparation method for the catalyst-assisted solvent-free ROP of TAH and the resulting polymer structure. The catalysts refer to Zn(DTC)₂, Na(DTC), or DTC with 1 to 10% molar ratios of TAH monomers. (**B**) Photograph of the resulting supramolecular materials. (**C**) Photograph showing the robust H-bonding network of a poly(TAH)-5% Zn(DTC)₂ sample (60 mm × 10 mm × 2 mm), which can support a 200-g weight without visible deformation. (**D**) Partial IR spectra of poly(TAH) polymers with and without different catalysts (5% mol ratio of TAH monomers). (**E**) Representative stress-strain curves of the poly(TAH) and poly(TAH)-5% Zn(DTC)₂ network in this work compared with the poly(TA-DIB-Fe) network in our previous study (*19*, *21*). (**F**) Comparison of Young's modulus and toughness of the poly(TAH) and poly(TAH)-5% Zn(DTC)₂ network compared with the poly(TA-DIB-Fe) network (*19*, *21*). (**G**) Representative tensile stress-strain curves of the processed filaments of poly(TAH) samples with 5% molar ratio of Zn(DTC)₂, Na(DTC), and DTC catalysts, respectively. The inset photograph showed that a polymer filament (8.5 mg; diameter = 0.74 mm) can sustain a 200-g weight (23,000-fold compared to its own weight). (**H**) Radar map showing the remarkably enhanced mechanical performance by the formation of secondary H-bonding clusters using 5% Zn(DTC)₂ as the catalyst. (**I**) Ashby plot shows the mechanical properties of our materials compared with current engineering materials. (I) reproduced from (*28*). PVC, polyvinyl chloride; PP, polypropylene; PE, polythylene; PTFE, polytetrafluoroethylene; EVA, ethylene-vinyll acetate.

(*19*) and even higher than that of the network toughened by strong iron(III)-carboxylate complexes (Fig. 2E) (*21*). The stiffened network of poly(TAH) still retained good stretchability (over 200%), suggesting that the reticular H-bonding network of poly(TAH) can sustain high tension force and dynamically dissipate external mechanical energy. Moreover, introducing DTC-based catalysts further stiffened the poly(TAH) network (Fig. 2E and figs. S40 to S42). For example, the poly(TAH) network obtained with the Zn(DTC)₂ catalysts shows Young's moduli varying from 53.2 to 340.3 MPa, dependent on the amount of catalyst (Fig. 2E and fig. S40). Higher catalyst loading up

to 10% molar ratio of TAH produced materials with poorer mechanical performances, which may be explained as the loss of reticular H-bonds due to the ligand competition effect as a result of the presence of excess catalysts. Combining the fact that (i) all samples have similar vibration bands ($v_{C=O}$) in IR spectra (Fig. 2D), (ii) metal-free catalysts also show remarkable stiffening effects (fig. S42), and (iii) control experiments show that adding ZnCl₂ salts does not stiffen the network (fig. S43), it is evident that the possible strengthening contribution due to metal-acylhydrazine complexes can be excluded in our materials. Furthermore, the two amide analogs, i.e.,

TAA and TAMH, were polymerized under the same condition used for TAH (figs. S44 to S51). The melts of TAA recrystallized back to monomers after cooling down to room temperature (fig. S45), which may be due to the favored monomer formation instead of polymers, caused by the spatially separated disulfide rings in the solid state as observed in the crystal structures resulting from the distinct H-bonding array (fig. S20). Poly(TAA) polymers can be obtained by irradiating the melts of TAA in solvent-free state, but the resulting materials showed fragility and poor mechanical properties (fig. S47). The melts of TAMH were still flowing liquids after cooling (fig. S48), suggesting the lack of H-bonding cross-links. The addition of $Zn(DTC)_2$ can facilitate the curing of poly(TAMH) (figs. S49 and S50), and the resulting network exhibited very soft properties (Young's modulus = 0.83 MPa; fig. S51). Therefore, these results unambiguously indicate that the formation of the specifically designed reticular H-bond cross-links are responsible for the robustness enhancement of poly(TAH) materials.

Despite the high stiffness, the poly(TAH) network with 5% molar ratio $Zn(DTC)_2$ maintained good stretchability with a breaking elongation over 150%, meanwhile exhibited enhanced toughness up to 29.6 MJ/m^3. A comparison of the poly(disulfide) networks with different sidechain cross-link units unambiguously illustrates the discovered stiffening effect of the acylhydrazine units (Fig. 2F). The homogeneous H-bond cross-linking of acylhydrazine units enables a two-orders of magnitude stiffening effect compared with the corresponding carboxylic acids (19), and the secondary clustering H-bonding cross-linking can further stiffen the poly(TAH) network over 40 times. It should also be noted that the metal-free H-bonded network presented here exhibits three times higher toughness compared to the state-of-the-art poly(TA) materials cross-linked by iron-carboxylic ionic clusters (21). Further, speed-dependent tensile experiments indicated that the reticular H-bonding network of poly(TAH) materials can dissipate the mechanical energy and enable stretchability at different tensile speeds (10 to 100 mm/min) (fig. S52). The tensile experiments of the samples with a half-width notch further show the high toughness of the network (fig. S53).

Besides the mechanical robustness and toughness of the bulky materials, thin filaments can also be made by tension-induced fiber processing from the hot melt liquid of the poly(TAH) with catalysts, as a result of the dynamic covalent bonds in the main chain of poly(disulfides). The diameter of the filaments can be controlled by the tensile speed to produce thin filaments (fig. S54), indicating the processibility. The stress-strain curves of these filaments showed high and reproducible mechanical robustness and toughness similar to that of the bulk materials (Fig. 2G and figs. S55 to S58). As a visible illustration, a piece of filament with a diameter of 0.74 mm was used to successfully sustain the load of a 23,000-fold weight of itself (Fig. 2G and movie S2).

Combining all these properties and structural data, it has been unambiguously demonstrated that the introduction and control of the reticular H-bonding cross-links of acylhydrazine units can simultaneously stiffen, toughen, and strengthen the solvent-free poly(disulfide) polymer network (Fig. 2, F and H). The unique multiple H-bonding cross-linking of acylhydrazines featuring high density, oversaturation, and unprecedented geometrical synergy results in robust and tough supramolecular networks (see Fig. 2I for a comparison with common engineering materials) (28).

Dynamic functions

Supramolecular materials feature intrinsically dynamic functions, such as self-healing and reprocessing capabilities (29–32), however, in most cases, being a trade-off with mechanical robustness. A pertinent question is whether the stiffened supramolecular materials in our system still exhibit dynamic properties. We performed dynamic mechanical analysis (DMA) (fig. S59) and rheological analysis (Fig. 3A and fig. S60) to understand the temperature dependency of their mechanical properties (fig. S59). DMA data showed that poly(TAH) and poly(TAH)-5% $Zn(DTC)_2$ showed similar storage moduli (around 2 GPa) at the glassy state, and the T_g of poly(TAH)-5% $Zn(DTC)_2$ was higher than that of poly(TAH) (fig. S59). Both of poly(TAH) and poly(TAH)-5% $Zn(DTC)_2$ samples exhibited a typical rubbery plateau (Fig. 3A) with frequency dependency (fig. S60), indicating the existence of physical entanglements in the network. This observation is consistent with the literature (33), in which the thermal polymerization of 1,2-dithianes results in cyclic polymers with physical entanglements, which also contribute to the mechanical stretchability of the network. To quantify the temperature-dependent viscosity of the material, creep and relaxation experiments were performed at different steady temperatures (Fig. 3B and fig. S61). The poly(TAH)-5% $Zn(DTC)_2$ sample exhibited excellent creep resistant at ambient temperature (below 30°C), while its viscosity visibly decreased from 36 MPa·S (30°C) to 4 MPa·S (40°C), indicating the remarkably accelerated chain mobility at 40°C. These results indicated that despite the high stiffness of poly(TAH)-5% $Zn(DTC)_2$ network, chain mobility is still allowed under mild conditions.

To quantitatively understand the temperature-dependent chain mobility in the solvent-free H-bonding network, the apparent activation energy (E_a) of the supramolecular network was evaluated by a series of temperature-dependent relaxation experiments using rheometry (Fig. 3C and figs. S62 and S63). It was found that poly(TAH) without catalyst exhibited a linear relationship in the entire temperature region tested, and the E_a was calculated as 58 kJ mol^{-1}. The E_a of poly(TAH)-5% $Zn(DTC)_2$ materials showed strong temperature dependency: The E_a' below 40°C was as high as 251 kJ mol^{-1}, while it decreased to $E_a'' = 97$ kJ mol^{-1} above 40°C. The change of E_a should be related to the glass transition due to the observed T_g at 37.8°C (fig. S59). Realizing the fact that this material is chemically cross-linked by H-bonds, the chain mobility is dominated by the exchange of H-bonded pairs (17). These thermodynamic results can provide quantitative understanding for the temperature-dependent dynamic nature of the reticular H-bond cross-links. Therefore, the resulting network of poly(TAH)-5% $Zn(DTC)_2$ reached a subtle balance between robustness and dynamicity in the transition temperature region (25° to 40°C), which is reminiscent of ice, being simultaneously robust and plastic (24).

The unusual combination of chain mobility and robustness gave us the opportunities to explore the self-repairing properties of the material. A widely recognized evaluation method was used to reproducibly establish the self-repairing efficiency of stiff materials (17, 34). The self-repairing process of two solid samples was studied at a contacting interface through a hole of a Teflon membrane spacer under a constant temperature and compression force (see detailed experimental details in the "Experimental method" section in the Supplementary Materials), and the dependency of repairing efficiency as a function of both temperature and repairing time was investigated (Fig. 3D and fig. S64). The samples of poly(TAH)-5% $Zn(DTC)_2$ exhibited a tension strength of 12.4 MPa after repairing 6 hours at 40°C and were fully repaired (over 20 MPa) after 48 hours at 40°C. As expected, decreasing the repairing temperature to 30°C led to a lower repairing efficiency (~75%) in 48 hours. The temperature dependency of the self-repairing efficiency in this material was consistent
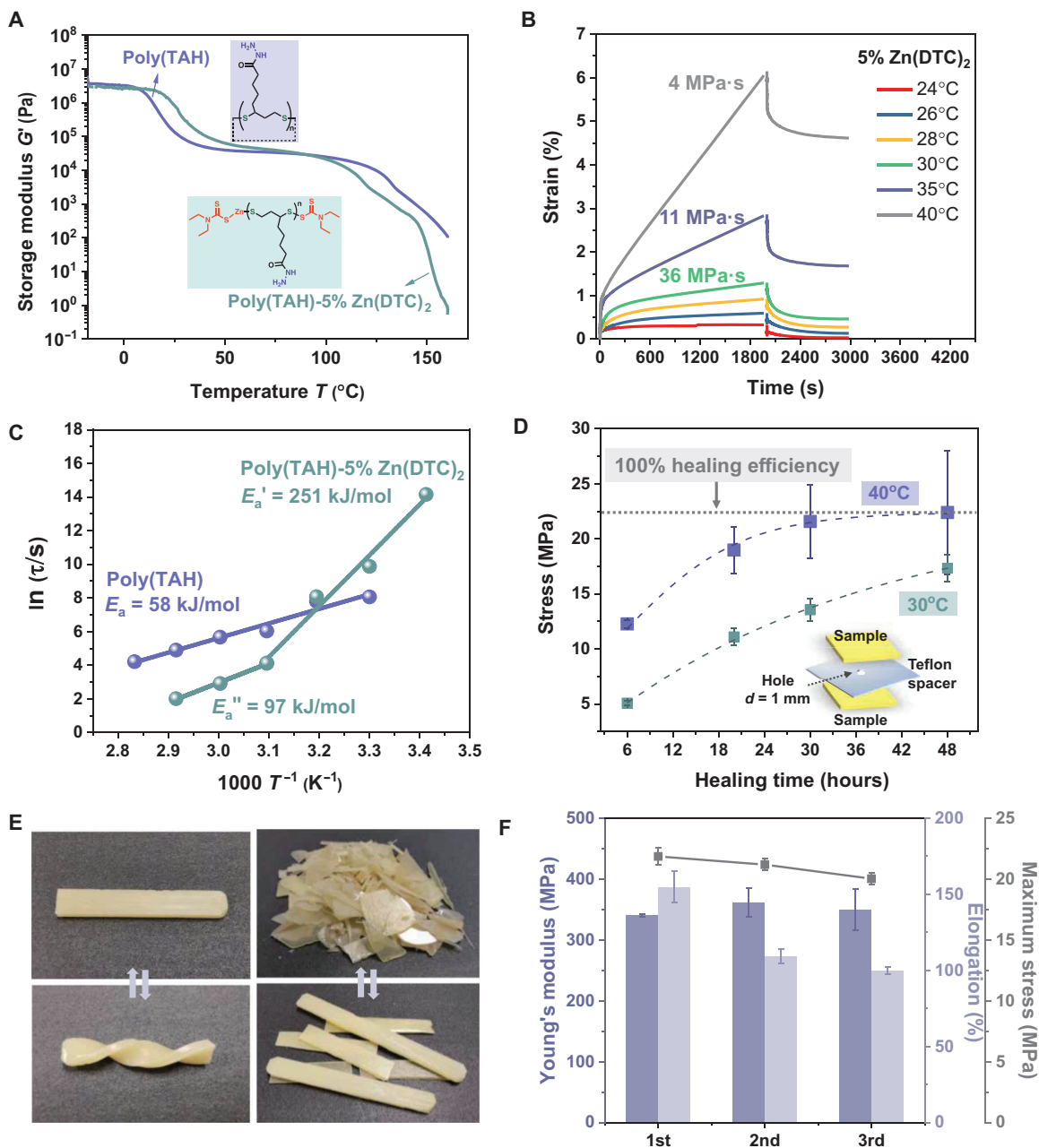
Fig. 3. Dynamic properties and functions enabling malleability, repairability, and recyclability. (**A**) Temperature-dependent storage moduli of poly(TAH) with and without 5% Zn(DTC)$_2$ catalyst recorded by rheometer under a constant frequency of 1 Hz. (**B**) Creep-recovery plots for poly(TAH)-Zn(DTC)$_2$ at different temperatures under 10 KPa. Viscosity is calculated and marked to quantify the temperature-dependent chain mobility. (**C**) Arrhenius plot of the poly(TAH) with and without 5% Zn(DTC)$_2$ catalyst. The relaxation time at different temperature is collected on the basis of the rheology master curves with different reference temperature (fig. S62) or the temperature-dependent stress relaxation curves (fig. S63). A notable slope increase is observed in the plot of poly(TAH)-5% Zn(DTC)$_2$ below 40°C, indicating the remarkable stiffening of the materials due to the formation of reticular H-bond clusters. (**D**) Time-dependent repair strength of the interacted samples through the hole of a Teflon membrane at 30°C and 40°C. The strength of the completely repaired sample was evaluated as 22 MPa by hot pressing the interfaces at 100°C for 3 hours. (**E**) Reprocessability of the stiff and dynamic supramolecular materials by readily shaping or pressing at mild conditions (45°C). (**F**) Mechanical performances of the reprocessed poly(TAH)-5% Zn(DTC)$_2$ materials after repeating multiple cycles.

with the results demonstrated by creep and relaxation experiments. Taking advantages of the readily malleable and repairable ability of our materials, further experiments showed that the mechanical robust supramolecular materials can be reshaped under mild heating conditions, resulting in a spiral material with persistent shape at

room temperature (Fig. 3E). Meanwhile, polymer fragments can be reprocessed into renewed plastic materials by hot pressing at 50°C. The "recycled" materials showed remaining microphase structures and similar mechanical performance over several cycles (Fig. 3, E and F, and fig. S65). These results demonstrated the advantageous nature

of the intrinsic and robust cross-links due to the reticular H-bonds of acylhydrazines and the distinctive dynamic behavior in the solvent-free network of dynamic poly(disulfides).

Interfacial adhesion ability

The supramolecular materials based on poly(TAH) also exhibited great potential as high-performance hot melting adhesive materials. One of the drawbacks of commercially available macromolecular adhesives rests on the low penetration ability of long polymers on widely used rough surfaces (35–37), which might lead to the existence of many bubbles or the presence of solvents between the adhesion interfaces. We anticipated that the small-molecule precursor of our materials can readily penetrate the surfaces and form molecule-level noncovalent interactions, such as H-bonds and metal-ligand interactions (Fig. 4A). Then, the formation of reticular H-bonding cross-links after cooling to room temperature produced a robust polymer adhesion layer, without the use of external additives, such as water needed for cyanoacrylate-based adhesives (38). We discovered that the formed adhesion layers using poly(TAH) can sustain unexpectedly high loading forces for glass and aluminum surfaces, both of which are important substrates for engineering adhesives (Fig. 4, B and C, and movie S3).

To quantitatively evaluate the adhesion strength of our materials, a widely applied lap shearing testing method was used, and the shearing adhesion strength of all poly(TAH) with or without catalysts was systematically investigated (Fig. 4D): The average adhesion strength of poly(TAH) without catalysts was as high as 11 MPa for aluminum surfaces, which was even fourfold higher than the maximum adhesion strength of poly(TA-DIB-Fe) copolymers based on our previous work (19). This enhancement was notable when realizing that the current system was free with any metal ions or covalent cross-linkers and can be attributed to the robust cross-linking interactions of acylhydrazines. Furthermore, the adhesion strength for aluminum surfaces can be further increased to 18 ± 3 MPa in the presence of poly(TAH)-2% Zn(DTC)$_2$. Next, a series of different surfaces were used to evaluate the general adhesive ability of the material (Fig. 4E). Compared with representative commercial hot melt adhesives (39), the adhesive strength of our materials was over 5.1-fold higher on glass, 16.0-fold higher on aluminum, 10.1-fold higher on fiberglass, and comparable on other surfaces. The high adhesive performance is attributed to the combined effect of (i) high penetration ability of small-molecule precursors that enables molecule-level contact, (ii) the robust and tough supramolecular polymer network cross-linked by the reticular H-bonds, and (iii) the noncovalent interactions between
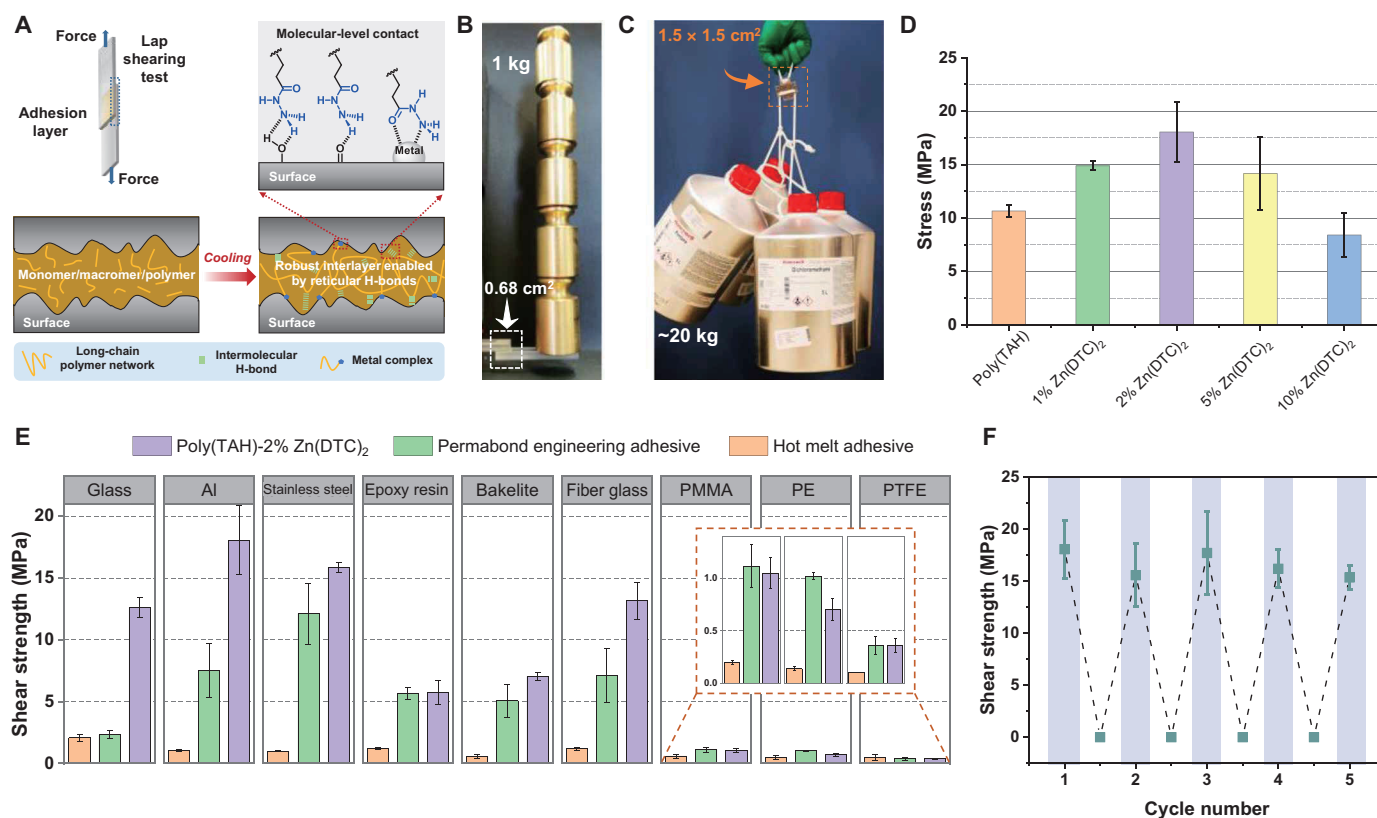

Fig. 4. Interfacial adhesion strength of the reticular H-bonding network. (**A**) Schematic representation of the adhesion behavior of traditional macromolecular adhesives and the solvent-free small-molecule adhesives. (**B** and **C**) Photographs showing the robust adhered glass surfaces (B) and aluminum surfaces (C). The loading experiment of 20-kg weights is recorded by video (movie S3). (**D**) The shear strength of the resulting materials using different amounts of Zn(DTC)$_2$ catalysts. (**E**) The shear strength of poly(TAH)-2% Zn(DTC)$_2$ for a variety of surfaces compared to two types of commercial adhesive materials, including Permabond engineering epoxy adhesive and poly(ethylene-vinyl acetate) hot melt adhesive. Al, aluminum. (**F**) Recyclable adhesive ability of the resulting materials on aluminum surface showing no fatigue after multiple heating/cooling cycles. PMMA, polymethyl methacrylate.

the acylhydrazine groups and the interfacial metal atoms or functional groups, such as hydroxyl groups and carbonyl groups. Moreover, due to the inherently reconfigurable poly(disulfide) main chain, our adhesive materials can be repeatedly used for multiple adhesive cycles without any fatigue (Fig. 4F). The high adhesive ability together with the excellent recyclability endows these poly(TAH) materials with the capability to form the basis for next-generation supramolecular adhesives made from biobased small molecules (35).

In conclusion, we demonstrated a robust supramolecular cross-linking strategy by simply converting carboxylic acids into acylhydrazines. By elaborating the reticular H-bonding cross-links of acylhydrazine units in a solvent-free poly(disulfide) network with dynamic covalent bonds, these supramolecular materials show excellent mechanical properties with simultaneously two or three orders enhanced stiffness, they are significantly toughened, meanwhile exhibiting readily repair properties and malleability under mild conditions while exhibiting strong adhesion and recyclable adhesive abilities. Noting the widespread use of polymers containing carboxylic acids and esters, it can be expected that our approach allows a general and versatile cross-linking strategy for designing supramolecular materials combining robustness, dynamic properties, and recycling capacities and offers ample opportunities to design future long-range ordered robust supramolecular materials and circular plastics.

MATERIALS AND METHODS

Polymerization procedure
In a typical procedure, 5 g (0.023 mol) of TAH monomer was added into a 15-ml Teflon vial, which was then heated by a metal heating block with a constant temperature of 145°C. Yellow viscous liquid TAH was obtained under magnetic stirring. In the case of catalytic polymerization, a given amount of catalyst was added as powder into the molten TAH liquid and dissolved by vigorous stirring. Next, the reaction mixture was stirred at 145°C for 2.5 hours to obtain homogeneity, and the resulting liquid was quickly transferred into a Teflon mold and cooled to room temperature to form free-standing polymer samples.

Tensile testing
All the tensile tests were carried out on an Instron 4301 tensile machine mounted with a maximum 5 KN detection cell. The data were recorded in real time by a wire-connected computer system. Unless otherwise noted, samples were tested at a fixed tensile speed of 10 mm/min. Tensile bars (60 mm by 5 mm by 2 mm) were prepared using a Teflon mold with multiple cells to enable parallel conditions. Tensile measurement was carried out at ambient condition for all samples, and each measurement was repeated with at least three independent samples.

Healing testing
The tensile tests for self-healing samples were conducted on an Instron 5565 tensile machine with a 100 N detection cell. Two 1-mm-thick poly(TAH)-5% Zn(DTC)$_2$ rectangular sheets (5 mm by 5 mm) were examined at a contacting interface through a hole of a Teflon membrane spacer (diameter = 1 mm; fig. S64). The assembled specimens were put in an oven with a given constant temperature under a constant compression force (1 MPa) for different healing time. Then, the repaired sandwich-like specimens were glued to the surface of aluminum plates, which were measured by the tensile machine at a testing speed of 10 mm/min.

Adhesion testing
Adhesion tests were performed at room temperature on an Instron 4301 tensile machine mounted with a 5 KN load cell. The polymers were molten into low-viscosity liquid by heating at 145°C and then deposited on the surfaces to adhere two surfaces together after cooling down to room temperature. The adhered samples were fixed to the jigs of the tensile machine to measure the shear strength of the adhesion layer. In the case of glass surfaces, special ultrastrong glass plates were used to be able to sustain the shearing force due to the high adhesion strength of the adhesive interfaces.

REFERENCES AND NOTES

1. J. R. Jambeck, R. Geyer, C. Wilcox, T. R. Siegler, M. Perryman, A. Andrady, R. Narayan, K. L. Law, Plastic waste inputs from land into the ocean. *Science* **347**, 768–771 (2015).
2. Science to enable sustainable plastics, *A White Paper from the 8th Chemical Sciences and Society Summit (CS3)* (2020).
3. A. H. Tullo, Plastic has a problem; is chemistry the solution? *Chem. Eng. News* **97**, 29–34 (2019).
4. C. Fouquey, J. M. Lehn, A. M. Levelut, Molecular recognition directed self-assembly of supramolecular liquid crystalline polymers from complementary chiral components. *Adv. Mater.* **2**, 254–257 (1990).
5. T. Aida, E. W. Meijer, S. I. Stupp, Functional supramolecular polymers. *Science* **335**, 813–817 (2012).
6. S. Wang, M. W. Urban, Self-healing polymers. *Nat. Rev. Mat.* **5**, 562–583 (2020).
7. P. R. Christensen, A. M. Scheuermann, K. E. Loeffler, B. A. Helms, Closed-loop recycling of plastics enabled by dynamic covalent diketoenamine bonds. *Nat. Chem.* **11**, 442–448 (2019).
8. Z. Zou, C. Zhu, Y. Li, X. Lei, W. Zhang, J. Xiao, Rehealable, fully recyclable, and malleable electronic skin enabled by dynamic covalent thermoset nanocomposite. *Sci. Adv.* **4**, eaaq0508 (2018).
9. J. B. Zimmerman, P. T. Anastas, H. C. Erythropel, W. Leitner, Designing for a green chemistry future. *Science* **367**, 397–400 (2020).
10. J.-M. Lehn, Dynamers: Dynamic molecular and supramolecular polymers. *Prog. Polym. Sci.* **30**, 814–831 (2005).
11. S. J. Rowan, S. J. Cantrill, G. R. Cousins, J. K. Sanders, J. F. Stoddart, Dynamic covalent chemistry. *Angew. Chem. Int. Ed.* **41**, 898–952 (2002).
12. D. B. Amabilino, D. K. Smith, J. W. Steed, Supramolecular materials. *Chem. Soc. Rev.* **46**, 2404–2420 (2017).
13. P. R. Chivers, D. K. Smith, Shaping and structuring supramolecular gels. *Nat. Rev. Mat.* **4**, 463–478 (2019).
14. L. E. Buerkle, S. J. Rowan, Supramolecular gels formed from multi-component low molecular weight species. *Chem. Soc. Rev.* **41**, 6089–6102 (2012).
15. R. P. Sijbesma, F. H. Beijer, L. Brunsveld, B. J. Folmer, J. K. Hirschberg, R. F. Lange, E. W. Meijer, Reversible polymers formed from self-complementary monomers using quadruple hydrogen bonding. *Science* **278**, 1601–1604 (1997).
16. B. J. Folmer, R. P. Sijbesma, R. M. Versteegen, J. A. J. Van der Rijt, E. W. Meijer, Supramolecular polymer materials: Chain extension of telechelic polymers using a reactive hydrogen-bonding synthon. *Adv. Mater.* **12**, 874–878 (2000).
17. Y. Yanagisawa, Y. Nan, K. Okuro, T. Aida, Mechanically robust, readily repairable polymers via tailored noncovalent cross-linking. *Science* **359**, 72–76 (2018).
18. C. G. Salzmann, P. G. Radaelli, A. Hallbrucker, E. Mayer, J. L. Finney, The preparation and structures of hydrogen ordered phases of ice. *Science* **311**, 1758–1761 (2006).
19. Q. Zhang, C. Y. Shi, D. H. Qu, Y. T. Long, B. L. Feringa, H. Tian, Exploring a naturally tailored small molecule for stretchable, self-healing, and adhesive supramolecular polymers. *Sci. Adv.* **4**, eaat8192 (2018).
20. Q. Zhang, Y. X. Deng, H. X. Luo, C. Y. Shi, G. M. Geise, B. L. Feringa, H. Tian, D. H. Qu, Assembling a natural small molecule into a supramolecular network with high structural order and dynamic functions. *J. Am. Chem. Soc.* **141**, 12804–12814 (2019).
21. Y. Deng, Q. Zhang, B. L. Feringa, H. Tian, D. H. Qu, Toughening a self-healable supramolecular polymer by ionic cluster enhanced iron-carboxylate complexes. *Angew. Chem. Int. Ed.* **59**, 5278–5283 (2020).
22. Q. Zhang, Y. Deng, C. Y. Shi, B. L. Feringa, H. Tian, D. H. Qu, Dual closed-loop chemical recycling of synthetic polymers by intrinsically reconfigurable poly(disulfides). *Matter* **4**, 1352–1364 (2021).

23. C. Y. Shi, Q. Zhang, B. S. Wang, M. Chen, D.-H. Qu, Intrinsically photopolymerizable dynamic polymers derived from a natural small molecule. *ACS Appl. Mater. Interfaces* **13**, 44860–44867 (2021).

24. U. Schmidt, P. Grafen, H. W. Goedde, Chemistry and biochemistry of α-lipoic acid. *Angew. Chem. Int. Ed.* **4**, 846–856 (1965).

25. S. H. Gellman, G. P. Dado, G. B. Liang, B. R. Adams, Conformation-directing effects of a single intramolecular amide-amide hydrogen bond: Variable-temperature NMR and IR studies on a homologous diamide series. *J. Am. Chem. Soc.* **113**, 1164–1173 (1991).

26. P. J. Nieuwenhuizen, A. W. Ehlers, J. G. Haasnoot, S. R. Janse, J. Reedijk, E. J. Baerends, The mechanism of zinc (II)-dithiocarbamate-accelerated vulcanization uncovered; theoretical and experimental evidence. *J. Am. Chem. Soc.* **121**, 163–168 (1999).

27. C. Hilger, R. Stadler, New multiphase architecture from statistical copolymers by cooperative hydrogen bond formation. *Macromolecules* **23**, 2095–2097 (1990).

28. M. F. Ashby, The CES EduPack database of natural and man-made materials, in *Cambridge University and Granta Design* (2008).

29. M. Burnworth, L. Tang, J. R. Kumpfer, A. J. Duncan, F. L. Beyer, G. L. Fiore, C. Weder, Optically healable supramolecular polymers. *Nature* **472**, 334–337 (2011).

30. P. Cordier, F. Tournilhac, C. Soulié-Ziakovic, L. Leibler, Self-healing and thermoreversible rubber from supramolecular assembly. *Nature* **451**, 977–980 (2008).

31. M. W. Urban, D. Davydovich, Y. Yang, T. Demir, Y. Zhang, L. Casabianca, Key-and-lock commodity self-healing copolymers. *Science* **362**, 220–225 (2018).

32. Y. Yang, M. W. Urban, Self-healing polymeric materials. *Chem. Soc. Rev.* **42**, 7446–7467 (2013).

33. K. Endo, T. Yamanaka, Copolymerization of lipoic acid with 1, 2-dithiane and characterization of the copolymer as an interlocked cyclic polymer. *Macromolecules* **39**, 4038–4043 (2006).

34. F. Maes, D. Montarnal, S. Cantournet, F. Tournilhac, L. Corté, L. Leibler, Activation and deactivation of self-healing in supramolecular rubbers. *Soft Matter* **8**, 1681–1687 (2012).

35. C. Y. Shi, Q. Zhang, H. Tian, D.-H. Qu, Supramolecular adhesive materials from small-molecule self-assembly. *SmartMat* **1**, e1012 (2020).

36. C. Heinzmann, C. Weder, L. M. de Espinosa, Supramolecular polymer adhesives: Advanced materials inspired by nature. *Chem. Soc. Rev.* **45**, 342–358 (2016).

37. S. Dong, J. Leng, Y. Feng, M. Liu, C. J. Stackhouse, A. Schönhals, L. Chiappisi, L. Gao, W. Chen, J. Shang, L. Jin, Z. Qi, C. A. Schalley, Structural water as an essential comonomer in supramolecular polymerization. *Sci. Adv.* **3**, eaao0900 (2017).

38. H. W. Coover, D. W. Dreifus, J. T. O'connor, Cyanoacrylate adhesives, in *Handbook of adhesives* (Springer, 1990), pp. 463–477.

39. S. Ebnesajjad, A. H. Landrock, *Adhesives Technology Handbook* (William Andrew, 2014).

Acylhydrazine-based reticular hydrogen bonds enable robust, tough, and dynamic supramolecular materials

Yuanxin DengQi ZhangChenyu ShiRyojun ToyodaDa-Hui QuHe TianBen L. Feringa

View the article online
https://www.science.org/doi/10.1126/sciadv.abk3286
Permissions
https://www.science.org/help/reprints-and-permissions

Use of think article is subject to the Terms of service